Schweizerische Eidgenossenschaft
Confédération suisse
Confederazione Svizzera
Confederaziun svizra

Federal Department of the Environment, Transport, Energy and Communications DETEC

Swiss Federal Office of Energy SFOE
Energy Research and Cleantech Division

REEL Demo – Romande Energie ELectric network in local balance Demonstrator

Deliverable: 3Overall Cross-site Comparison of the performance of different DSM strategies. Investigation of the possible conflicts (LIC and Chapelle-sur-Moudon) and sub-optimality issues.

Demo site: Chapelle

Developed by
Lorenzo Nespoli, ISAAC, SUPSI
Vasco Medici, ISAAC, SUPSI
Davide Strepparava, ISAAC, SUPSI
Roman Rudel, ISAAC, SUPSI

[Canobbio, 25.03.2021]

1 Description of deliverable and goal

This deliverable focuses on the comparison of distributed demand-side management (DSM) strategies in two different demo sites. The focus is on the comparison of the results, by means of simulations, of the Lugaggia Innovation Community (LIC) and the "REseaux en Equilibre Local" (ReEl) demo sites.

1.1 Executive summary

In this deliverable, we simulated the outcome of applying different distributed DSM algorithms using advanced forecasting models in two demo sites: LIC [1], a self-consumption community located in Lugaggia, a small village near Lugano, and the ReEl demo site, located in Chapelle-Sur-Moudon. The simulations used the best forecaster method selected from D1.2.5a-b, Chapter(s) on the design and test of distributed DSM algorithms that use communication and new forecasting models. The two demo sites are different in size and scope. While the LIC demo site is a self-consumption community, the ReEL demo is composed of a private battery and a district battery operated to perform peak shaving. In the LIC case, a distributed control can be applied to model the costs of the LIC community with an automated market making mechanism (AMM) and solving the associated Nash Equilibrium, as described in D1.2.5a-b. On the other hand, in the ReEL demo, no obvious business model can be applied to coordinate the two installed batteries, which have clearly different and possibly competing objectives. We then use a lexicographic approach to allow cooperative coordination, ensuring that the privately owned battery does not degrade its economic performances due to coordination. We compare this kind of coordination with other types of control strategies to investigate the existence of win-win coordination strategies.

1.2 Research question

- What is the economic impact, for the end users, of control strategies in different demo sites?
- What kind of distributed control algorithms can be adopted for different business models?
- What market designs can be adopted to prevent active agents in the network from having conflicting economic goals and, if this cannot be avoided, what control strategies can be adopted?

1.3 Novelty of the proposed solutions compared to the state-of-art

In this deliverable we compare the distributed control algorithm developed during the REeL project, which are beyond the state of the art, in closed-loop

[1] https://lic.energy/

control, for different grid topology and use cases. We analyze the results by means of techno-economic KPIs.

1.4 Description

1.4.1 Demo site description

In the following, we summarize the setting and the characteristics of the two demo sites.

LIC LIC is a self-consumption community, which consists of the following components:

- 18 single-family houses with 4 PV power plants, for a total of 37 kWp
- A kindergarten with
  - A roof-mounted 27 kWp PV power plant
  - A 50kW / 60kWh community battery installed in the basement and operated by the administrator of the community (AEM)

In the actual pilot project, the total installed PV power is 64kWp. With respect to the original configuration, the PV power was increased by an additional 33kWp, in order to simulate a likely future situation, justifying the use of local storage. The loads and PV plants characteristics were reconstructed based on the data originally provided by the local DSO. The LIC's grid topology is shown in figure 1.

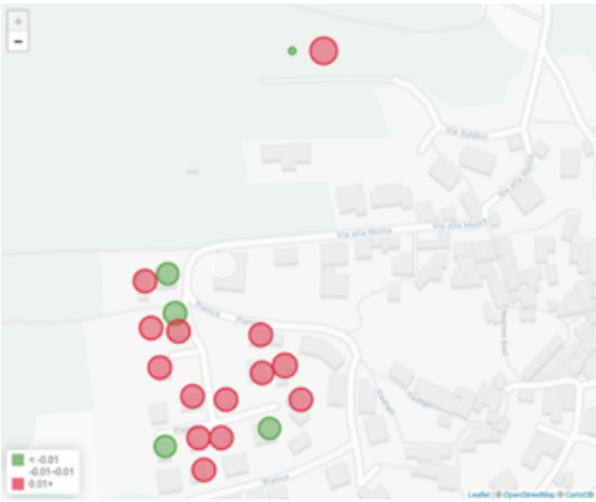

Figure 1: The LIC demo site

ReEL The ReEL demo site consists of a grid of LV grid of Chapelle-Sur-Moudon. A total of 7 nodes are monitored, shown in figure 2. A total of 3 batteries are installed in the grid, two of which can be directly controlled:

- Node 100: a 300 kWh district-level battery with charging and discharging power of [50, -200] kW located at the PCC. It is intended to be used for peak shaving to smooth the consumption peak and reduce the production peaks generated by the PV power plants.
- Node 107: a 40 kWh battery with charging and discharging power of [10, -20] kW is owned by an end-user and is operated to maximize self-consumption and minimize its billing costs.

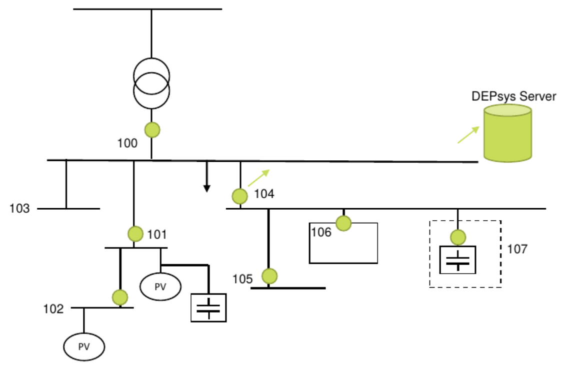

Figure 2: The ReEL demo site

1.4.2 Control strategies

LIC In the LIC community, a local energy market and a local flexibility market (LEM and LFM, respectively) are in place. They are both implemented in the form of dynamic prices with functional dependence on the instantaneously produced or consumed energy inside the local grid. This kind of price formation mechanisms is also known as automated market making mechanism (AMM). The LEM prices are generated by a simple set of rules:

$$\begin{aligned} p_b &= \left(E_c p_b^{BAU} - \min(E_c, E_p)(p_b^{BAU} - p_b^{P2P})\right)/E_c \\ p_s &= \left(E_p p_s^{BAU} - \min(E_c, E_p)(p_s^{P2P} - p_s^{BAU})\right)/E_p \end{aligned} \tag{1}$$

where p_b and p_s are the buying and selling prices generated by the AMM, E_c and E_p are the sum of the energy consumed and produced inside the energy community, while p_b^{BAU}, p_s^{BAU}, p_b^{P2P} and p_s^{P2P} are the buying and selling prices in the Business as Usual (BAU) case and inside the energy community. In such a pricing configuration, peers clearly profit from the difference in price between BAU and P2P, but the community administrator also earns money when energy is self-consumed inside the community. It is important to notice that the P2P tariff is applied only to the energy produced by the members of the community. As a consequence, it is also in the administrator interest to maximize self-consumption (no conflicting interests between peers and community admin). Instead of directly minimizing the prices in equations (1), we decided to minimize the surplus function $e(u)$, which is the surplus that the agent community has in paying the energy at the point of common coupling with the electrical grid:

$$e(x) = c\left(\sum_{i=1}^{N} u_i\right) - \sum_{i=1}^{N} c(u_i) \tag{2}$$

where $u_i \in \mathbb{R}^{\mathrm{T}}$ is the vector of total power of the ith agent, $c(\cdot)$ is the energy cost function defined as:

$$c(p_t) = \begin{cases} p_{b,t}^{BAU} p_t, & \text{if} \quad p_t \geq 0 \\ p_{s,t}^{BAU} p_t, & \text{otherwise} \end{cases} \tag{3}$$

where $p_{b,t}^{BAU}$ and $p_{s,t}^{BAU}$ are the buying and selling tariffs, respectively, at time t. Minimizing $e(u)$ maximizes the self-consumption of the EC, and thus indirectly minimizes the costs defined in (1). The overall objective function for the end users (not including system-level constraints) becomes:

$$\begin{aligned} c_{tot}(u_i, u_{-i}) &= c_i(u_i) + \alpha_i e(u) \\ &= \alpha_i c\left(\sum_{i=1}^{N} u_i\right) + (1-\alpha_i) c(u_i) \end{aligned} \tag{4}$$

where α is a repartition coefficient for prosumer i. Jointly minimizing (4) induces a game with unique generalized variational equilibrium [1], which can be reached using the preconditioned forward backward formulation [2]. Refer to D1.2.5a-b for more details. The batteries are coordinated in a model predictive control (MPC) fashion: at each step they coordinate through the preconditioned forward backward algorithm iteratively, solving several instances of their optimization problem. This routine is then repeated in the next time step (15 minutes). We here describe the battery optimization problem. Called $u = [p_{ch}^T, p_{ds}^T]^T \in \mathbb{R}^{2T}$ the vector of concatenated decision variables for the control horizon T, where p_{ch} and p_{ds} are the battery charging and discharging power, respectively, $\tilde{u} = [p_{ch}, p_{ds}] \in \mathbb{R}^{T\times 2}$ being the same vector reshaped in a 2 columns matrix, $\hat{p} \in \mathbb{R}^T$ being the forecasted power at household's main for the next control horizon, $y \in \mathbb{R}^T$ being an auxiliary variable representing the users' costs $c(u_i)$, the batteries solve the following MIQP problem:

$$u^*, y^*, s^* = \underset{u,y,s}{\operatorname{argmin}} \quad \alpha_i \nabla c\left(\sum_{i=1}^{N} u_{i,pre}\right)^T u_i + (1-\alpha_i)\sum_{i=1}^{T} y + \rho_d \|u - u_{pre}\|^2 \tag{5}$$

$$x_{t+1} = Ax_t + B\tilde{u}^T \tag{6}$$

$$y \succcurlyeq p_b\left(\tilde{u}[1,-1]^T + \hat{p}\right) \tag{7}$$

$$y \succcurlyeq p_s\left(\tilde{u}[1,-1]^T + \hat{p}\right) \tag{8}$$

$$x \in [x_{\min}, x_{\max}] \quad u \in [u_{\min}, u_{\max}] \tag{9}$$

$$p_{ch} \preccurlyeq s u_{max,ch} \quad p_{ds} \preccurlyeq (1-s) u_{max,ds} \tag{10}$$

where $\succcurlyeq$ stands for $\succcurlyeq_{R_+}$, indicating element-wise inequalities, $p_b \in \mathbb{R}^T$ and $p_s \in \mathbb{R}^T$ are the business as usual buying and selling prices, $u_{i,pre}$ are the agents actions at the previous iteration and $x_{\min}, x_{\max}, u_{\min}, u_{\max}$ are operational limits. Here s is a binary variable which prevents the battery to simultaneously charge and discharge, which makes the overall problem mixed integer. More details on the role of y, the dynamics equation and the proximal term $\rho_d\|u - u_{pre}\|^2$ can be found in D1.2.5a-b. In addition, the LFM can be activated by the DSO in case in which the power at the PCC exceeds some critical values., The LFM has a similar dynamic price formulation, and has the purpose of promoting peak shaving. The LFM price, which is additional to the LEM prices, can be expressed as:

$$c_{LFM} = \beta P_{PCC} p_i \tag{11}$$

where β is a tunable parameter in $[CHF/kWh^2]$. This can be readily added to the end users' objective function, so that the resulting objective function would be:

$$\alpha_i \nabla c \left(\sum_{i=1}^{N} u_{i,pre} \right)^T u_i + (1 - \alpha_i) \sum_{i=1}^{T} y + \rho_d \|u - u_{pre}\|^2 + \beta P_{PCC,pre} u \tag{12}$$

For comparison, we also simulated the case in which constraints on the maximum power at the PCC are explicitly taken into account. This is done including the box constraint $P_{PCC} \in [P_{PCC,min}, P_{PCC,max}]$ in the total cost using a Lagrangian relaxation, such that the final total cost can be written as:

$$\alpha_i \nabla c \left(\sum_{i=1}^{N} u_{i,pre} \right)^T u_i + (1 - \alpha_i) \sum_{i=1}^{T} y + \rho_d \|u - u_{pre}\|^2 + \lambda^T u \tag{13}$$

and where λ is updated using a standard ADMM formulation. More details on this approach can be found in [3, 1].

ReEL In the ReEl demo, the privately owned battery (the small one) has no economic reason to synchronize with the district level battery to perform peak shaving. In fact, the objective of the private battery is to increase its own self-consumption. However, typically, several equivalent solutions for the charging and discharging operations exist, which achieve the same results in terms of self-consumption. A win-win solution is to use a lexicographic approach for the small battery: at first, an optimal scheduling for the small battery, which maximizes its owner's self-consumption, is obtained, u^*_{sc}. This optimal scheduling generates the cost $c(u^*_{sc})$ and the final state of charge of the battery, x^*_T. These can be used as constraints during coordination. $c(u^*_{sc})$ is used to define an upper bound for the small battery cost, which cannot be increased while helping the big battery in peak shaving activities. x^*_T is used to prevent the small battery from discharging only to reduce the aggregated peak. The initial optimization problem can be formulated as:

$$u^*_{sc}, y^*_{sc}, s^*_{sc} = \underset{u,y,s}{\text{argmin}}\ c(u) \tag{14}$$
$$s.t.\ \ (6-10) \tag{15}$$
$$\tag{16}$$

where $(6-10)$ is the set of constraints described above. The initial optimization problem is solved at the beginning of each coordination step. Then, the following optimization problem is solved for each iteration of the coordination process:

$$u^*, y^*, s^* = \underset{u,y,s}{\text{argmin}}\ c(u) + \beta P^T_{PCC,pre} u + \rho_d \|u - u_{pre}\|^2 \tag{17}$$
$$s.t.\ \ (6-10) \tag{18}$$
$$c(u) \preccurlyeq c(u^*_{sc}) + \delta_c \tag{19}$$
$$x_T \succcurlyeq x^*_T - \delta_x \tag{20}$$

where u_{pre} are the battery operations at the previous iteration, δ_c and δ_x are small constants allowing little deviations from the solutions of the initial problem in terms of final user's costs and final state of charge. The expression $P^T_{PCC,pre}u$ is simply the linearization of the quadratic punishment on the the total power at PCC centered on the previous iteration, that is:

$$\left(\nabla_{u_{pre}} \frac{1}{2} \beta \|P_{PCC}(u_{pre})\|_2\right)^T u \tag{21}$$

It can be noted that the peak shaving cost is exactly equivalent to the formulation of the LFM prices for the LIC demo.

The nominal power of installed and simulated PV power plants, the number and characteristics of the batteries and the control strategies are summarized in table 1 for the LIC and REeL demo sites.

1.4.3 LIC: Numerical simulations

The grid of the neighbourhood that participates in the LIC project has been mapped, and its components simulated for the month of July. The grid topology and the characteristics of loads and PV plants were reconstructed based on the data ini-

	PV	Controllable batteries	Objective	Control type
LIC	97 kWp	4 x 15 kWh [-7, 7] kW	cost reduction using LIC prices	distributed
ReEl	200 kWp	40 kWh [-20, 10] kW 300 kWh [-200, 50] kW	Cost reduction Peak shaving	distributed, lexicographic

Table 1: Technical characteristics of the demo sites

tially provided by the local DSO. At the same time, the power flow was simulated using OpenDSS. Please refer to deliverable 1.2.5d for a detailed description of the simulation environment. We simulated three scenarios:

1. *Baseline*: no batteries
2. *LEM + grid constraints*: batteries coordinate to minimize the LEM prices, using (13) as objective function
3. *LEM + LFM*: batteries coordinate to minimize the LEM and LFM prices, using (12) as objective function

Grid analysis For the grid constraint, the two limits for the maximum positive and negative power at the coupling point were chosen based on an estimate of how much could ideally be steered using the available batteries if one had perfect forecasts. The limits have been selected based on a baseline simulation of the energy community without batteries. The limits have been selected to be as low as possible, given that the following two criteria are respected:

- The maximum daily energy exceeding the positive and negative limits must be smaller than the total energy storable in the batteries. This assumption means that in the worst day, all the batteries should have been empty (respectively full) to fulfil negative (respectively positive) grid constraints.
- The difference between the minimum limit and the quantile 0.01 of the power at the coupling point and between the quantile 0.99 of the power at the coupling point and the maximum limit must be smaller than the maximum charge and discharge power of the batteries, respectively.

Among the PCC's power density distribution, these limits are shown in detail for the month of July in the following figure. We stress that these limits were chosen automatically based on yearly simulation in which no devices were controlled.
The purpose of these simulations is to see the LFM price structure's effectiveness over explicitly integrating grid constraints into the distributed control problem. In figure 4, the effect on the PDF of the power at the LIC's PCC is shown for the three cases. In both the controlled instances, the batteries successfully shrink the PDF towards zero. It is also interesting to see how, for the case in which grid constraints where explicitly considered, the limits set on the PCC power were not respected. This can be explained as the effect of the imperfect energy forecasts: the Lagrangian multipliers handling grid constraints are non-zero only in cases in which their violations are correctly forecasted. On the other hand, adding a quadratic punishment further shrinks the distribution towards zero; since the presence of this quadratic term is not dependent on the quality of the forecasts, batteries can manage to shrink the tails of the power distribution further.

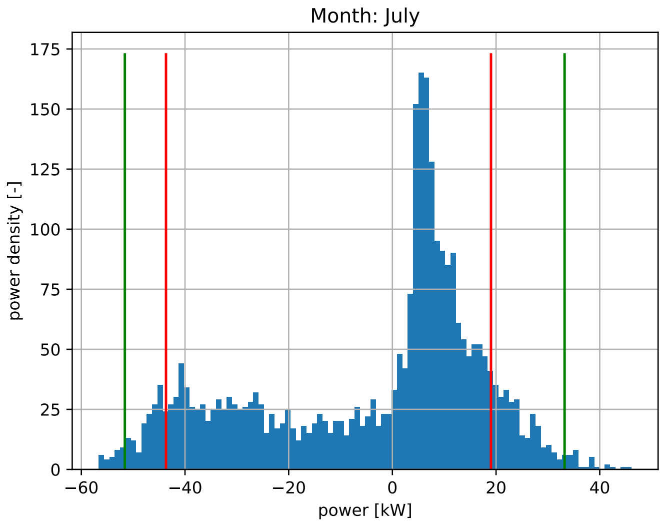

Figure 3: Power limits for the simulated month of July. Blue bars: histogram of the active power at the coupling point of the community. Green vertical lines: quantiles 0.01 and 0.99. Red bars: selected negative and positive power limits (-43.67kW and 19.02kW, respectively).

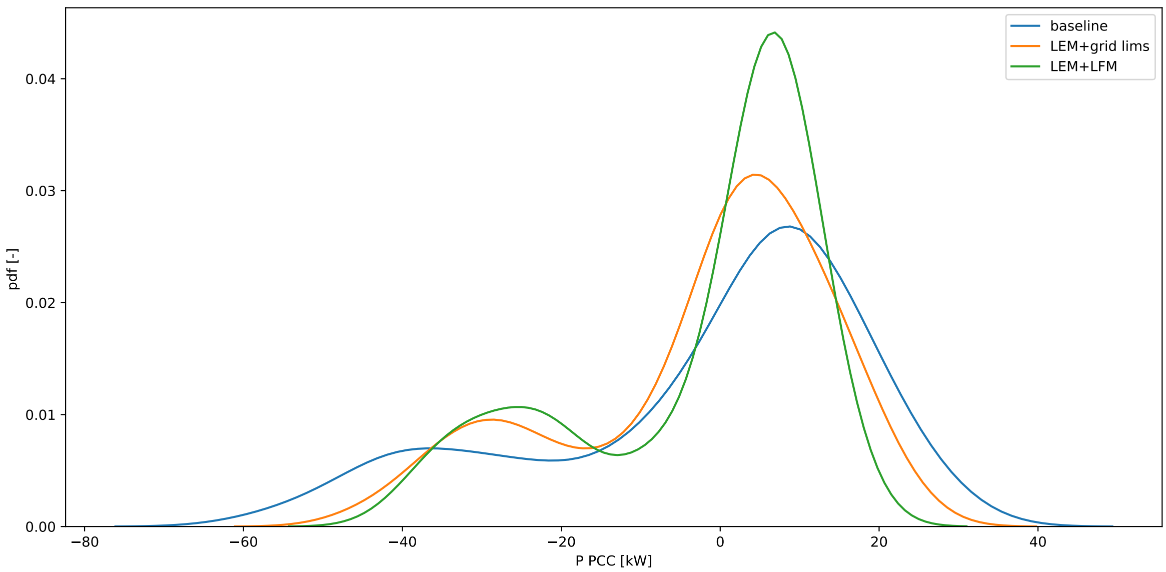

Figure 4: Probability density function (PDF) of the PCC's power for the baseline, with coordination, LEM prices and and explicit grid limits, and with LEM and LFM prices.

Economic analysis In this section, we evaluated the effect of the parameters of the LEM and LFM prices on the overall energy costs for end-users. Figure 5 shows the effect of changing p_b^{P2P}, p_s^{P2P} and the LFM quadratic parameter β on the final costs for the LIC end users, without controlling any device. The costs are computed using one-year real data from the pilot site for 2020. The p_b^{BAU} and p_s^{BAU} are fixed to the DSO prices for LIC, which are 6 and 21 CHF cts/kWh, respectively. In the next figure, p_b^{P2P}, p_s^{P2P} are jointly changed between 8-10 and 14-18 CHF cts, respectively, when LFM is not active. The effect on the users' yearly costs is shown in term of yearly bonus, i.e. cost reduction w.r.t. the BAU case. We recall that when only LEM is active, all the users always have a net benefit. The left panel shows the yearly bonus for users without a roof-mounted PV power plant. In this case, their yearly bonus is not affected by the value of p_s^{P2P}, as we would expect. On the other, linearly decreasing the p_b^{P2P} linearly increases the bonus. For those users having a PV, the right panel shows that the effect of p_s^{P2P} is predominant over p_b^{P2P}. As most of the users don't have a PV power plant in LIC, energy production is still a scarce resource, and users who can sell energy have a higher economic bonus.

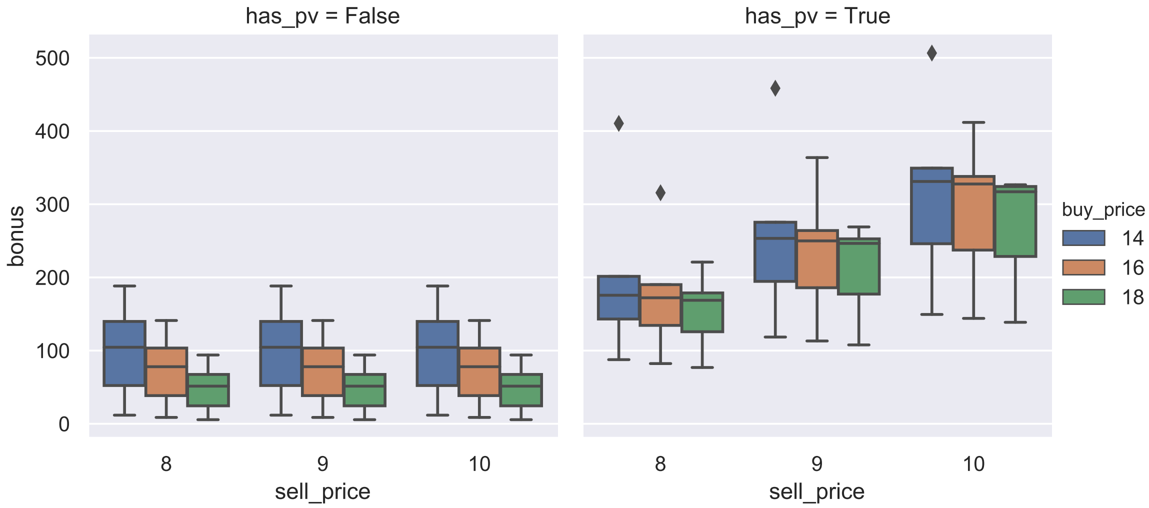

Figure 5: Effect of different p_b^{P2P}, p_s^{P2P} LEM prices on the final yearly cost for the end-users. Boxplots contain differences w.r.t. BAU. Left: users without roof-mounted PV power plants, right: with.

Figure 5 shows the same sensitivity analysis in terms of percentages. While the users without PV have a bonus in the range of 1-6% of their yearly consumption, the range for PV owners is substantially higher, up to 12%. The higher outlier is the kindergarten, in which only the community PV is present.

Figure 7 shows the effect of the LFM β [cts/kWh²] parameter on the yearly savings in terms of CHF, grouped by PV owners or net consumers. We fixed p_b^{P2P}, p_s^{P2P} to 16 and 9 cts, respectively. As previously explained, the LFM pricing scheme doesn't guarantee a cost reduction for end-users, as is the case for the LEM prices scheme. On the contrary, the LFM mechanism applies a bonus-malus scheme depending on the current contribution of the end users in shrinking the overall power profile to zero; as such, we can expect that for high values of β some users face a cost higher than the BAU case. As this is not desirable, the β parameter must be tuned for the specific market to which it is applied. This can be done in silico, based on historical production and consumption data, as in this case.

In this situation the PV owners are less penalized by the increase of the LFM β parameter, since energy production is the scarce resource inside the market. The converse is true when we look at simulation cases, in which, we recall, additional 33kWp of roof-mounted PV plants where installed. Under this condition, in the

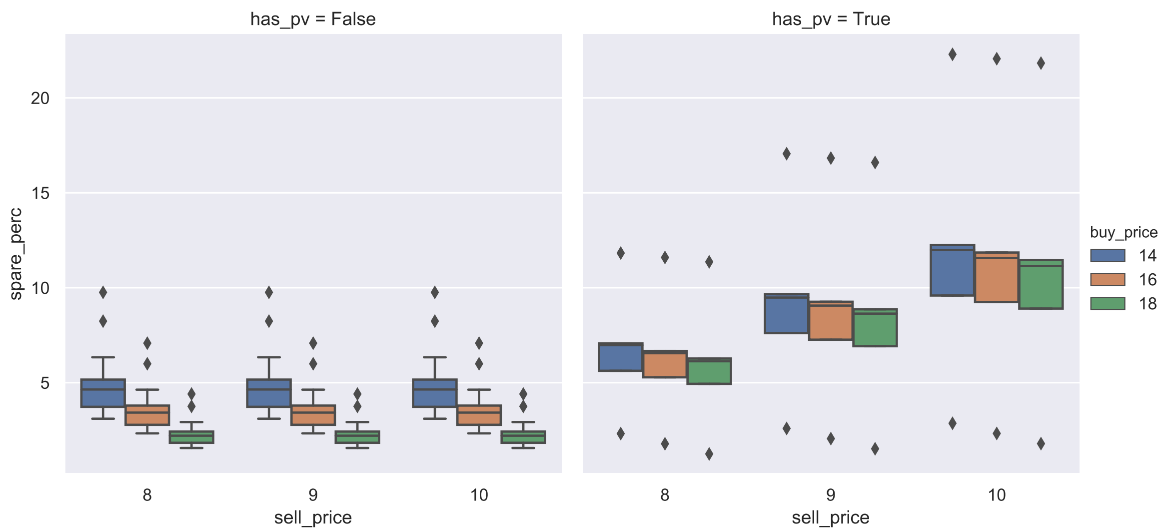

Figure 6: Effect of different p_b^{P2P}, p_s^{P2P} LEM prices on the final yearly cost for the end-users, as percentages

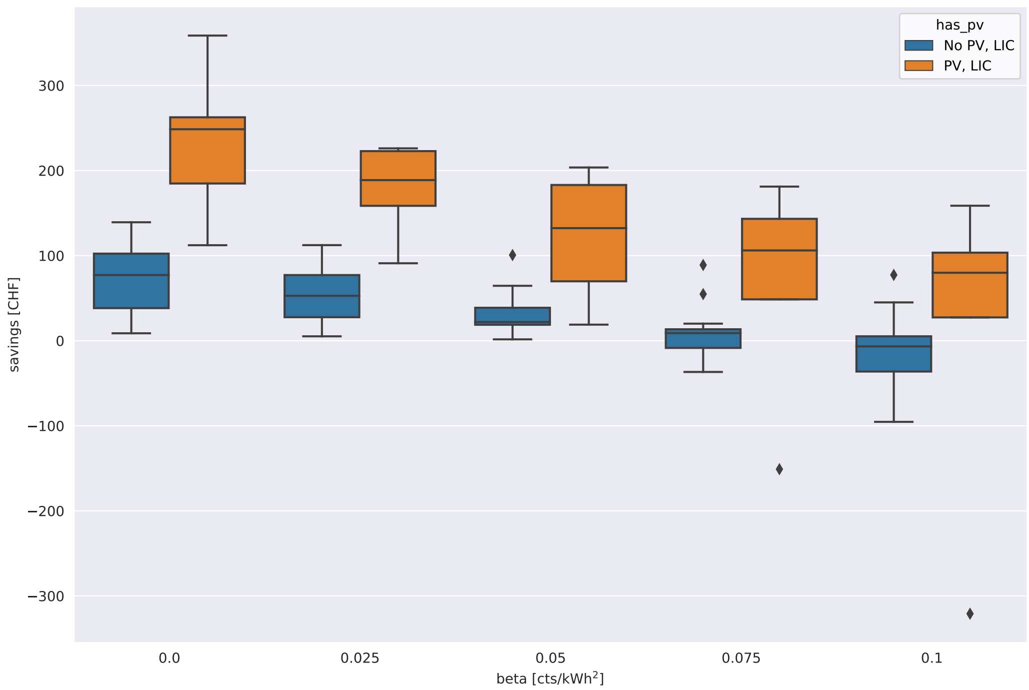

Figure 7: Effect of different values for the LFM parameter on the final yearly cost for the end-users. Boxplots contain differences w.r.t. BAU.

month of July we have an overproduction from PV power plants, which leads to a decrease of savings in CHF for PV users, if they don't optimize their power profile curves considering the LFM prices. In the following figure, these use cases where considered:

- No control. Users without PV nor battery (blue), users with PV+ battery (orange)

- Self-consumption optimization. Users with PV + battery (red), optimize for their self-consumption. Other users (green) take no actions.
- LEM+LFM: Users with PV + battery (violet), optimize for the LEM + LFM prices. Other users (brown) take no actions.

In the case in which the LFM is not active (β=0), the first four cases are not significantly different, while the savings increase when batteries are operated in order to directly optimize for the LEM prices. We stress that, in this case, the benefit of doing so also affects users who do not possess a PV nor control a battery (violet boxplot). When the LFM is activated, at increasing values of beta, PV owners see a reduction of their savings. This is because of the overproduction of PV in July. On the other hand, users without PV nor batteries face no significant changes w.r.t. the case in which only the LEM is active. Finally, we see that when users with a controllable battery use it to optimize the actual LEM+LFM prices, they still increase their final savings, even for high values of β.

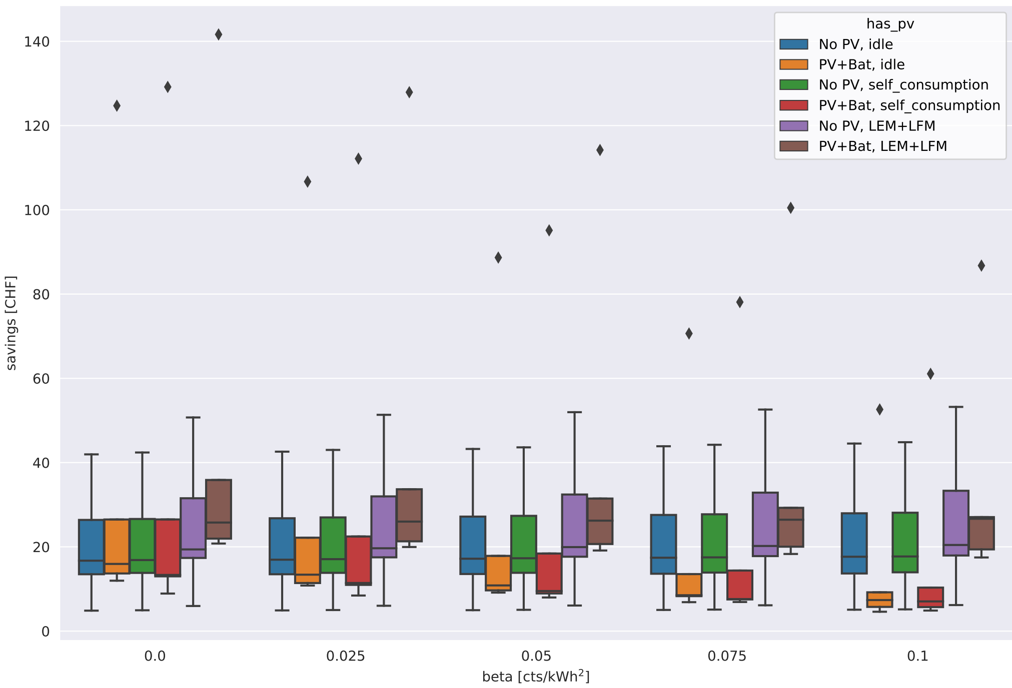

Figure 8: Boxplots of savings for the simulated month of July, for different use cases and groups of users. Blue, orange: no control, users with/without PV and battery. Green, red: self-consumption optimization, users with/without PV and battery. Violet, brown: LEM+LFM optimization, users with/without PV and battery.

1.4.4 ReEL: Numerical simulations

For the ReEL demo, we simulated the following scenarios, using the consumption and production data coming from the monitoring infrastructure described in section

1.4.1:

1. *baseline* - No batteries

2. *economic* - The small battery is operated to maximize its own self-consumption and thus to minimize its billing costs. The battery is charged as soon as production exceeds consumption and discharged as soon as consumption exceeds production. The district-level battery performs peak shaving.

3. *economic delayed charging*: The small battery is operated to maximize its own self-consumption and thus to minimize its billing costs. In this case, to minimize battery aging, we used a technique that attempts to minimize the average SOC over the control horizon. As a consequence, the battery is charged as late as possible and discharged as soon as possible. The district-level battery performs peak shaving.

4. *economic local peak shaving* - The small battery is operated lexicographically. At first, self-consumption is maximized, and the resulting projected costs are used as the upper boundary in the subsequent optimization, which applies a quadratic punishment to the power at the main of the building containing the battery to perform peak shaving. The district-level battery performs peak shaving.

5. *distributed control* - The small battery coordinate with the district-level one to perform peak shaving, using the lexicographic formulation introduced in section 1.4.2 and solving (18) at each iteration.

The simulations refer to the period from the 1st of September 2020 up to 31st of December 2020. Of this period, the first two weeks where only used to pre-train the forecasters, and are thus excluded from the final techno-economic analysis.

Grid analysis Figure 9 shows the density function of the power at the PCC (node 100), for the different simulated scenarios. While a significant difference in skewness is seen between baseline and the other three cases, no significant differences in power distribution are seen for the economic baseline, local and distributed control. This is because the district-level battery located at the PCC, which has a capacity of 7.5 times the small battery, is always operated with the sole objective of performing peak shaving. Figure 10 shows that the PDF of the power at the main connection point of the building containing the small battery is undoubtedly affected by the local control strategy, with the lexicography strategy that tends to tighten it. Nevertheless, the large battery can predict the transformer's power profile and compensate for its fluctuations in all cases with relatively similar performance.
A more detailed analysis on the effect of the two batteries in performing peak shaving can be done by plotting the boxplots of the power of the PCC, conditional to the quantile of the power of the considered battery (first panels of figure 11 and 12) and

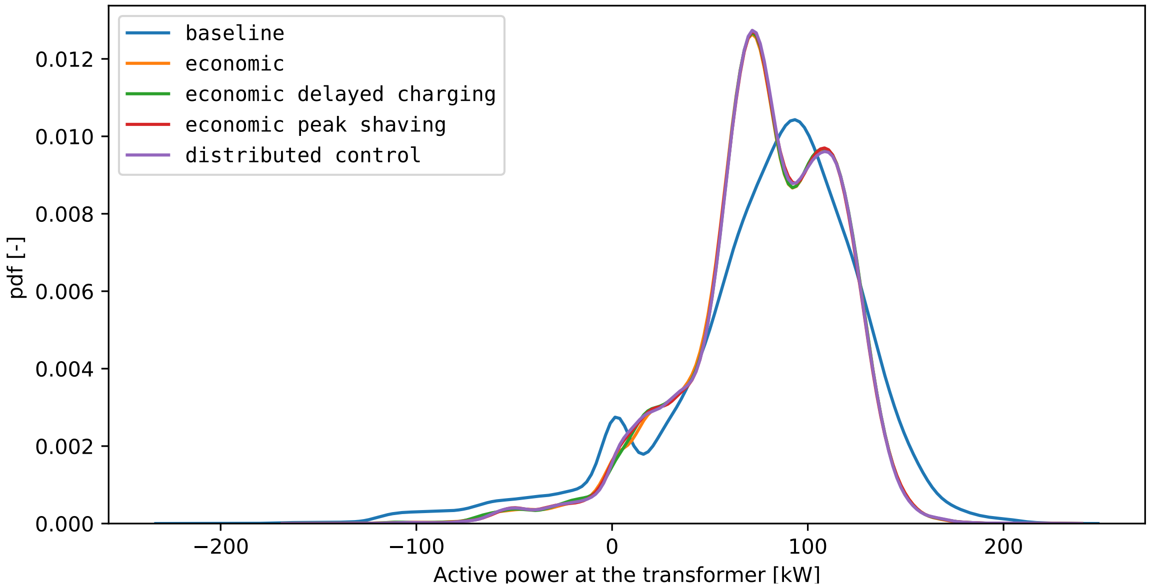

Figure 9: Probability density function of the power at the PCC, for the different simulated scenarios.

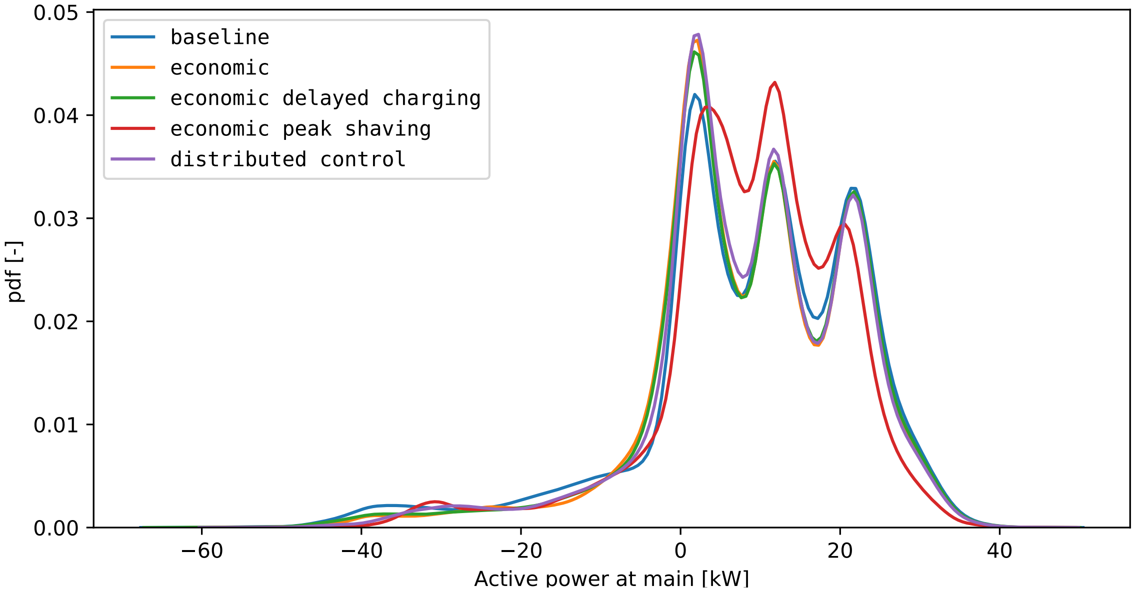

Figure 10: Probability density function of the power at the main of the building containing the small battery, for the different simulated scenarios.

vice versa (second panel of the same figures). For both batteries, the first panels of figure 11 and 12 show that the implemented strategies help to shrink the power distribution towards zero, especially for the extreme quantiles of the power of the batteries. Looking at the first quantile (0-0.01) of the power distribution of the batteries, the distributed control approach seems to perform slightly better in shrinking the lower tail of the power distribution at the PCC. No or very little differences between non-baseline cases are seen at the right tail of the distribution. Looking at the bottom panels of the two figures, we can see how in the economic baseline case, the small battery charges much less compared with the local peak shaving and distributed control cases, as expected (quantile 0-0.01, second panel of figure 11) while on the other hand, the district-level battery seems to compensate for this reduction in the same case (quantile 0-0.01, second panel of figure 12). Furthermore, it is clear that the small battery doesn't tend to charge while the power at the PCC is in the right tail of its distribution since the small, privately owned battery has no incentives in discharging into the grid.

Economic analysis Table 2 shows the two considered meters' economic results, 100 being the meter at the PCC where the district-level battery is located. For the latter, there is only a slight change in the final billing between those use cases where batteries are installed. This is mainly due to the fact that the district-level battery is always performing peak shaving (with or without coordination with the smaller battery) and has 7.5 times the capacity of the smaller battery. Focusing on the results of node 107, we see how the delayed charging slightly increases the total costs with respect to the simple economic strategy. Quite unexpectedly, actuating the battery using the lexicographic economic-peak shaving objective slightly reduces its billing costs with respect to the simple economic case. This is probably due to the imperfect forecasts: adding a peak shaving objective lexicographically, helps in mitigating forecasts errors, which may lead the battery to wrongly charge in periods with no production, or vice versa, discharge during non-consumption periods.

meter	b.	eco	eco-delay charg.	eco-peak sh.	distributed control
100	37994.1	37601.6	37601.4	37595.5	37598.0
107	5635.5	5384.7	5434.4	5377.0	5397.1

Table 2: Economic analysis for the two batteries

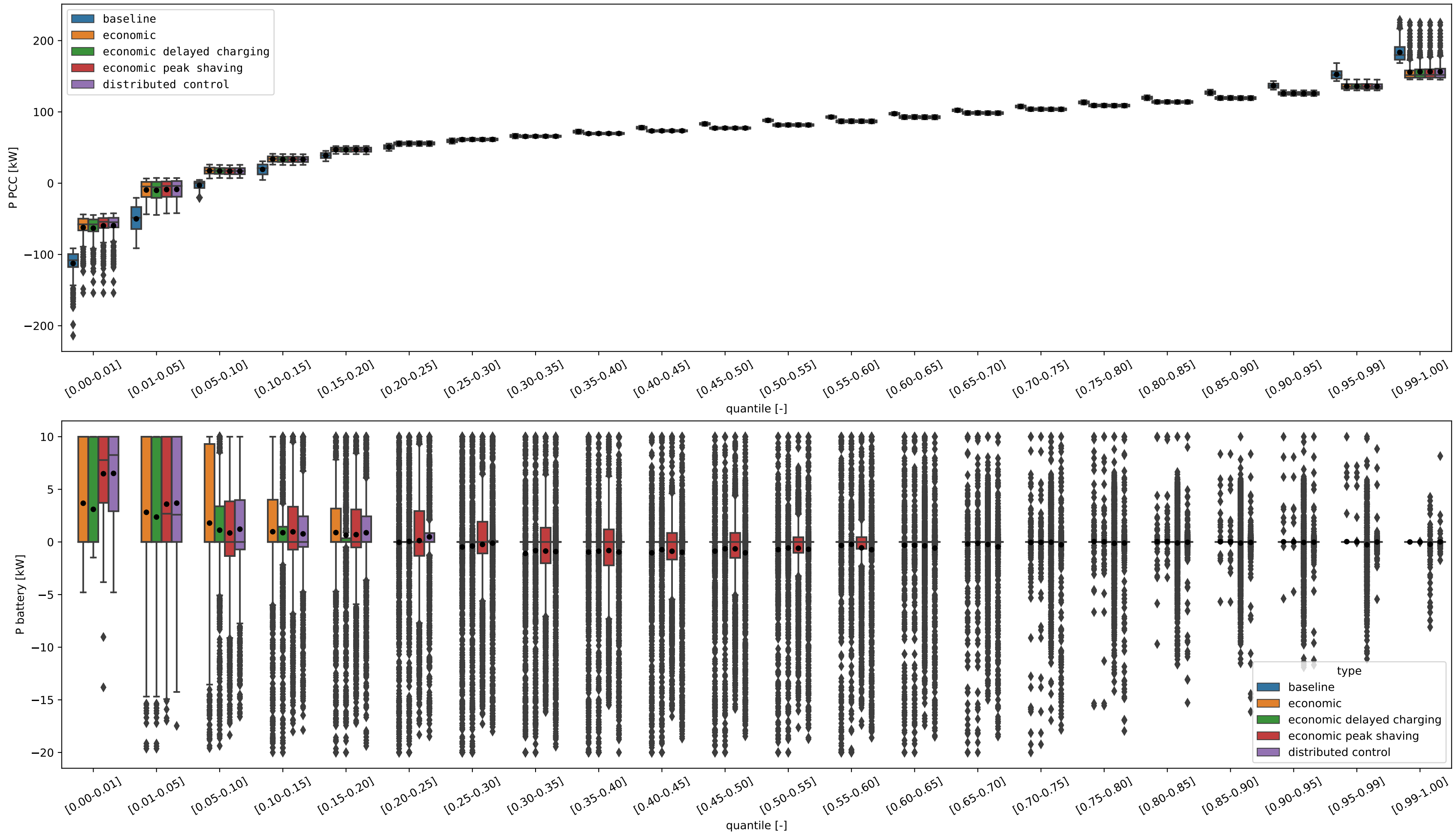

Figure 11: Effect of the small battery control on the power at the point of common coupling (PCC) of the community. Top: boxplots of the power at the PCC per inter-quantile range of battery's power. Bottom: boxplot of the battery power per inter-quantile range of the power at the PCC.

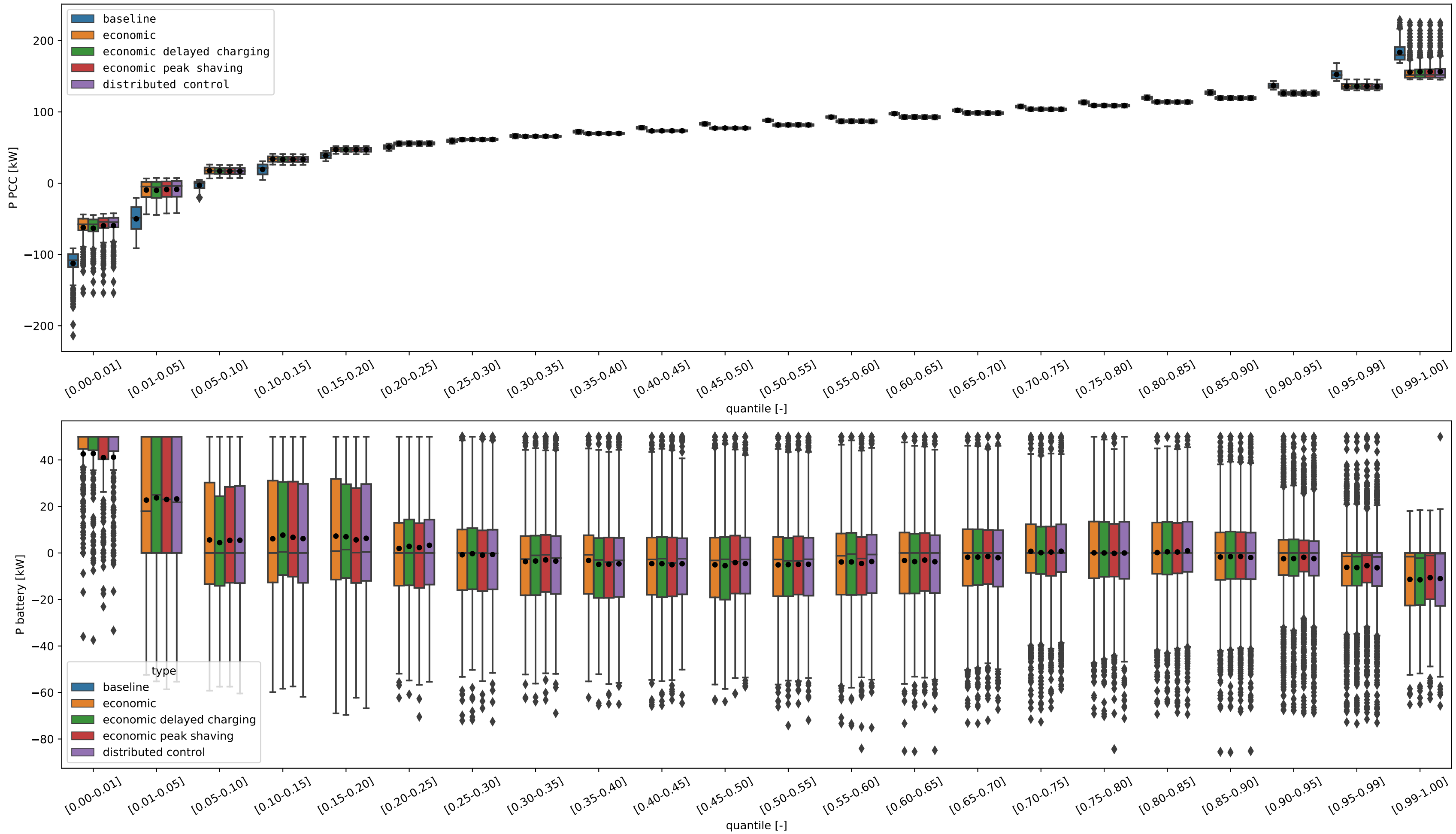

Figure 12: Effect of the district-level battery control on the power at the point of common coupling (PCC) of the community. Top: boxplots of the power at the PCC per inter-quantile range of battery's power. Bottom: boxplot of the battery power per inter-quantile range of the power at the PCC.

1.5 Regulatory and legal barriers for implementation

The AMM price formation scheme proposed for the LIC community generates costs that depend on the consumption of all the energy community participants. That is, it is not directly proportional to the energy consumed by the end user, and it gets lower when the self-consumption inside the energy community increases. Switzerland is embracing a causal principle on the price formation for end users, as stated in the recent modification to the Federal Electricity Supply Act [4]. This means that the electrical bills “should reflect costs caused by end users”. However, the Electricity Supply Ordinance [5] states that DSOs must guarantee to the end users that at least 70% of their bills are directly proportional to their energy use; at the same time they can offer opt-in tariffs in which this percentage is reduced. Under these constraints, the tariff proposed in 1.4.2 can be potentially applied in Switzerland. For the ReEL case, business as usual tariffs were considered, and no legal barriers are foreseen.

2 Achievement of deliverable

2.1 Date

March 2021.

2.2 Demonstration of the deliverable

This deliverable presents the impact of different control methods for DSM using communication and different forecasting models. The main features of the developed applications are presented in the previous sections.

3 Impact

This deliverable presents the results of applying different control and market mechanisms to two different demo sites. Namely, for the LIC demo site, an energy community with an AMM price formation scheme was simulated, and the effectiveness of distributed coordination among batteries was tested against simpler control strategies. Furthermore, a sensitivity study on the main parameters affecting the AMM and their effect on the aggregated power profile and on the end users’ bills was presented. A net benefit for the market participants is measured. Moreover, par-ticipants with highly controllable flexibility, such as batteries, can further optimize their cost-saving, even when the DSO imposes additional costs by activating the lo-cal flexibility market. For the ReEL demo site, in which no energy communities are present, we compared different control strategies of the sole privately owned battery, to assess to which extent its behaviour could influence the peak shaving operation of the DSO's owned district-level battery. Plausible control strategies were chosen among the ones minimally shifting the end user's costs from its optimal costs (obtained operating the battery to minimize self-consumption). Results show that, even if the different strategies result in substantially different scheduling for the privately-owned battery, the aggregate power distribution is marginally affected. This is to impute to the small size of the end-user battery compared to the district-level one.

References

[1] L. Nespoli, M. Salani, and V. Medici, "A rational decentralized generalized Nash equilibrium seeking for energy markets," in *2018 International Conference on Smart Energy Systems and Technologies, SEST 2018 - Proceedings*. Institute of Electrical and Electronics Engineers Inc., 10 2018.

[2] G. Belgioioso and S. Grammatico, "Projected-gradient algorithms for Generalized Equilibrium seeking in Aggregative Games are preconditioned Forward-Backward methods," *arXiv*, 2018.

[3] L. Nespoli and V. Medici, "Constrained hierarchical networked optimization for energy markets," in *Proceedings - 2018 IEEE PES Innovative Smart Grid Technologies Conference Europe, ISGT-Europe 2018*, 2018.

[4] "LAEI 734.7, https://www.admin.ch/opc/it/classified-compilation/20042411/index.html."

[5] "OAEI 734.71, https://www.admin.ch/opc/it/classified-compilation/20071266/index.html."